Radiography 31 (2025) 103020

Contents lists available at ScienceDirect

Radiography

journal homepage: www.elsevier.com/locate/radi

Development of populational female thorax sizes and body habitus categories using computed tomography (CT) images

R. Pape [a,*], G. Xie [b], X. Zheng [a], A. Carstens [c,d], C. West [e], C. Cowling [f]

[a] School of Dentistry and Medical Sciences, Discipline of Medical Radiation Science, Faculty of Science and Health, Charles Sturt University, Locked Bag 588, Building 30, Boorooma Street, Wagga Wagga, NSW, 2678, Australia
[b] Quantitative Consulting Unit, Office of Research Services and Graduate Studies, Charles Sturt University, Wagga Wagga, NSW, Australia
[c] School of Animal, Environment and Veterinary Sciences, Veterinary School, Charles Sturt University, Locked Bag 588, Wagga Wagga, NSW, 2678, Australia
[d] Companion Animal Clinical Studies, Faculty of Veterinary Science, University of Pretoria, Onderstepoort, South Africa
[e] Faculty of Science and Health, School of Nursing, Paramedicine and Healthcare Sciences, Charles Sturt University, Bathurst Campus, 353 Panorama Avenue, Mitchell, NSW, 2795, Australia
[f] Department of Medical Imaging and Radiation Sciences, School of Primary and Allied Health Care, Medicine, Nursing and Health Sciences, Monash University, Wellington Road, Clayton, VIC, Australia

ARTICLE INFO

Article history:
Received 31 January 2025
Received in revised form
14 June 2025
Accepted 19 June 2025
Available online xxx

Keywords:
Female thorax
Rib cage
Body habitus
Breast cancer
Mammography positioning
Bayesian network

ABSTRACT

Introduction: Positioning of the breast during mammography examination is critical to producing optimum quality images. However, the variation in female thorax and body habitus may affect mammography positioning for best image quality. This study aims to establish populational female thoracic (rib cage) sizes and quantify female body habitus categories.
Methods: A retrospective analysis of 347 female computed tomography (CT) chest axial scans was retrieved from an open access database to establish female rib cage sizes. Dimensions of the rib cage were measured digitally across six cross sections with six anterior rib landmark points and recorded in millimetres (mm). A Bayesian Network (BN) model was developed to establish the relationships of information extracted from the rib cage image data to quantify and categorise female body habitus.
Results: Female body habitus (thoracic size) were classified into three cohort categories: lean (20.5 %), norm (55.6 %) and curvaceous (23.9 %). The mean values (115–126 mm) and the corresponding 80 % prediction interval ranges for the healthy female rib cage size were obtained through the BN scenario analysis.
Conclusion: The significance of this study is that it categorised 55.6 % of female thoracic sizes as being normal on a larger group of female population. This study contributed to a good understanding of the range of female body habitus (thoracic size) to improve positioning practice and maximise image quality.
Implications for practice: This study used a BN model to establish a range of female thorax sizes using CT chest images to support improved positioning practices. These ranges of thorax sizes should be integrated as a body habitus criterion in the current image evaluation system to maximise image quality and subsequent breast cancer diagnosis.

Introduction

Breast cancer is a disease that causes deaths to millions of women worldwide. The incidence of breast cancer varies worldwide; it is the most common cancer diagnosed in females of all ages representing 1 in 4 cancers with an estimated number of more than 2 million (24.5 %) new cases in 2020.[1] Mammography is an imaging tool used to detect the early signs of breast pathology, including breast cancer. Mammography is accessed in two distinct settings: screening and diagnostic.[2] It can be used to screen women with no breast symptoms (asymptomatic), and secondly, it is used for diagnostic screening of women with breast symptoms (symptomatic). High quality mammography can be achieved at regular intervals through large scale organized screening programs in a healthy population of women.[3] This achievement has demonstrated successful early detection of breast cancer and

* Corresponding author.
E-mail address: rpape@csu.edu.au (R. Pape).

https://doi.org/10.1016/j.radi.2025.103020

reduced mortality and morbidity.[3] Men also can have access to diagnostic mammography services; however, breast cancer is not a common health issue among males.[4]

The two routine positioning techniques used to image the breast in both the screening and diagnostic settings worldwide are the craniocaudal (CC) view and the mediolateral oblique (MLO) view.[5] The breast is surrounded by a curvilinear thorax with breast tissue extending from the medial to lateral regions (Fig. 1). The axillary tail extends laterally and obliquely from the breast parenchyma of the upper outer quadrant (UOQ) into the axilla.[6] This confirms the evidence that a maximum breast parenchyma is located in the UOQ,[6] which is the region where majority of the breast cancer occurs.[3,6–9] The exclusion of breast tissue from the field of view of both the CC and MLO view may limit the opportunity to diagnose an early, potentially curable breast cancer.[10] Therefore, inclusion of the maximum amount of breast tissue as possible using both routine positioning techniques is significant in reducing the potential of missed breast cancers. However, factors such as the female thorax size and body habitus may impact on mammography positioning techniques.

Radiographers understanding of the human body habitus and its influence on positioning may assist in their decision making to maximise their positioning techniques. Radiographers' knowledge in adapting positioning techniques according to various body habitus should enable them to produce high quality images. Although body habitus may influence mammographic image quality (MIQ), obvious consideration of the impact on the size and shape of the thorax within the literature is limited.[12] Silent criteria have been identified as being used to assess MIQ and may be reflective of this understanding.[13] Radiography textbooks usually describe asthenic (tall persons with thin thoracic cages) and hypersthenic (shorter persons with wider thoracic cages) persons as the extremes within a population.[12,14] Both these body habitus may result in the need to repeat the images. The approximate percentage of the total human population for the four types of body habitus (asthenic, hypersthenic, sthenic and hyposthenic)[14] are shown in Fig. 2. The sthenic and hyposthenic persons reflect the average or 'normal' body habitus and may comprise broad shoulders and a developed chest.[14]

Although evidence reveals the impact of gender and underlying thoracic pathology,[15,16] blunt chest wall trauma[17] and surgical treatment of malignant thoracic wall tumours[15] on the size and shape of the thoracic wall, no identified literature relates these variations to mammographic practice. Importantly, there is no measurement of the female thorax and categories of female body habitus within a mammography screening population. This study aims to establish populational female thoracic (rib cage) sizes and quantify female body habitus categories using computed tomography (CT) images.

Method

The computed tomography (CT) chest images reviewed for this study were acquired using standard CT scanners (GE Medical Systems, Discovery CT750 HD). A retrospective analysis of a total of 347 de-identified female patient's CT non-contrast chest axial images aged 40–75+ were retrieved from the Medical Imaging and Data Resource Center (MIDRC) database[11] to establish the three female thorax sizes (small, average and large). The measurement of the length of the thorax using digital software (Digital Imaging and Communications in Medicine [DICOM]) format was adapted from the study methodology by Pickard et al.[18] Measurement of

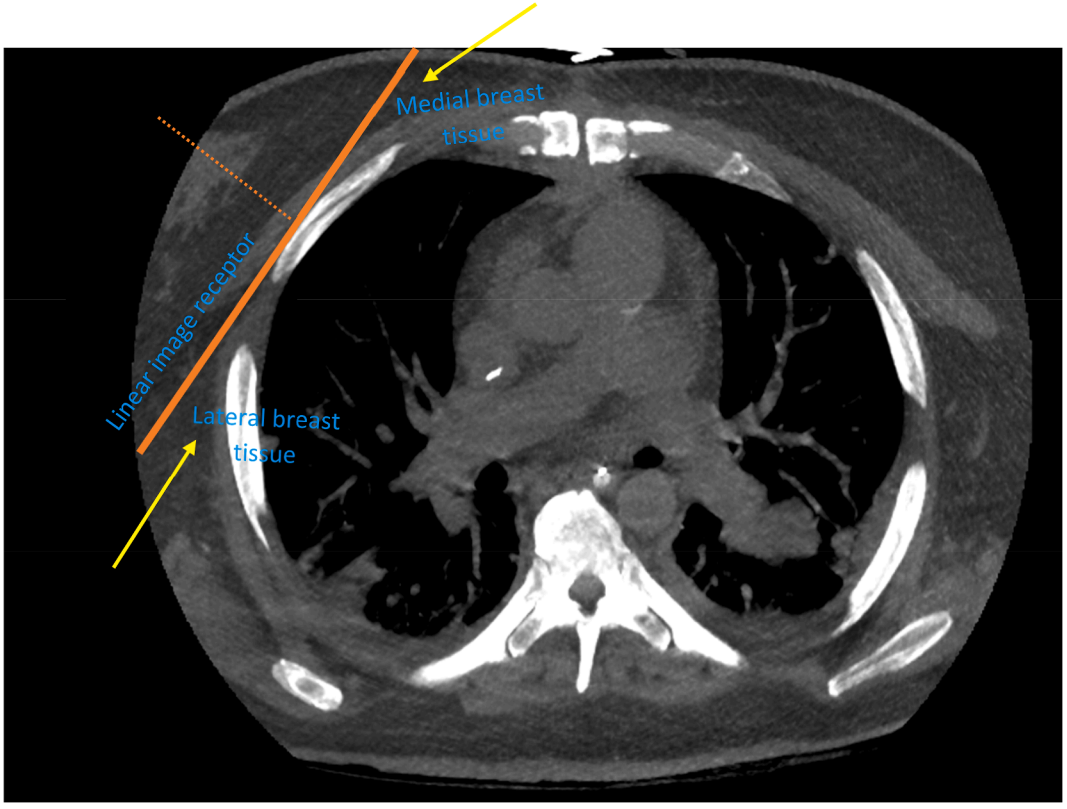

Figure 1. An axial computed tomography (CT) slice of the female thorax demonstrating the linear image receptor (orange thick) against the curved thorax. The missing lateral and medial breast tissue is arrowed (yellow). Source: CT chest data was obtained from the Medical Imaging and Data Resource Center (MIDRC) open access database.[11] (For interpretation of the references to color in this figure legend, the reader is referred to the Web version of this article.)

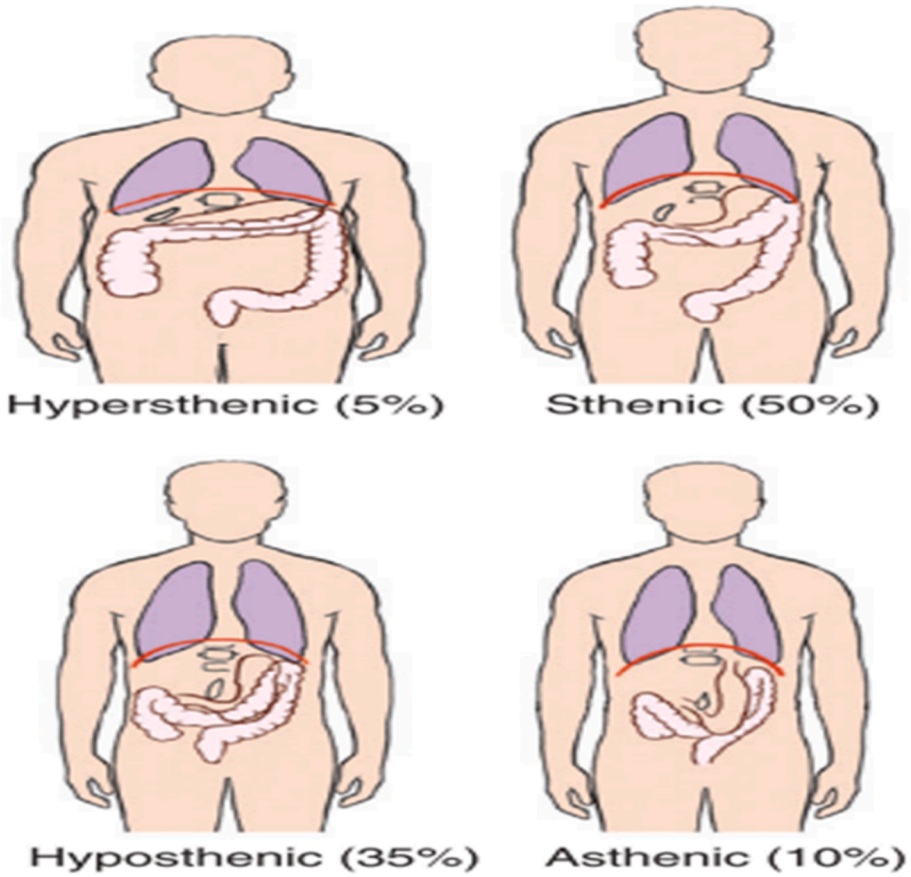

Figure 2. Four types of human body habitus. Source: Bontrager & Lampignano (2014).[14]

the thorax curvature adapted the methodology by Shi et al.,[19] including the baseline model using the rib landmark location and number distribution of ribs except the use of three-dimensional (3D) geometry model calculations as a potential limitation. Dimensions of the rib cage using digital ruler were manually measured across six cross sections with three anterior rib landmark points (RT Rib1, RT Rib2, RT Rib 3) on the right side of the sternum and three anterior rib landmark points (LT Rib1, LT Rib2, LT Rib3) on the left side of the sternum to determine the curvature of the thorax (Fig. 3). The mean values reflected an average (normal) female thoracic (rib cage) size, the minus two standard deviation (-2SD) values reflected the small (leaner) female anterior thoracic size and the plus (+) 2SD values reflected a large (curvilinear) female anterior thoracic size. All measurements were recorded in millimetres (mm) and rounded to the nearest one decimal place.

All CT chest images in DICOM format used in this research are in public domain and the accesses of these databases were approved by the database owners and their respective institutions.[11] Data access is free to registered users from academia and government. As such: (1). data analysed in this study was anonymised to protect patient identification and complied with data governance standards more robustly; and (2). informed consent was obtained prior to data collections by the respective database owners.[11]

BreastScreen Australia (BSA) recommends biannual screening of asymptomatic women aged 50–69 years.[20] However, women aged 40–49 years and 70 years and above are also able to access the screening program. The CT chest images reviewed in this study population reflected asymptomatic women aged 40 years or over. By using the open source DICOM viewer, the following characteristics of each variable were recorded: participants, image series, population, study year and age. Computed tomography (CT) chest images of female patients' aged 40–75+ were randomly selected in establishing a range of female thorax sizes. Personal information was limited to demographics including gender, age and ethnic population. From 2021 to 2022, there were 588,682 women aged 40–75+ years screened at BreastScreen (BS) NSW.[21] The ideal sample size of CT chest images of women based on 95 % confidence interval (CI) in this study was 384[22] and could reflect the BS NSW screening female population aged 40–75+[21]. Only 347 images were retrieved in this study with a minor difference of 37 ($n = 37$) to meet the requirement of 95 % CI and to validate statistical power of quantifying body habitus categories in a female screening population. CT images excluded from the study included patients' that have other chest pathologies, spinal trauma or rib anomalies,[15–17] pectus deformities,[23] congenital anomalies of the anterior thoracic wall,[24] pectus excavatum (depressed sternum),[16,25] male chests, and no age given.

Results

Raw data were collected and imported into Microsoft Excel for further analysis. Descriptive and exploratory statistical analyses were performed using the free professional Statistical software R (version 4.2.2)[26] for preparing the data for the development of the Bayesian network model.

Originally developed as a modelling tool from artificial intelligence since late 1980s, today Bayesian Networks (BNs) have found their applications range across the sciences, industries and

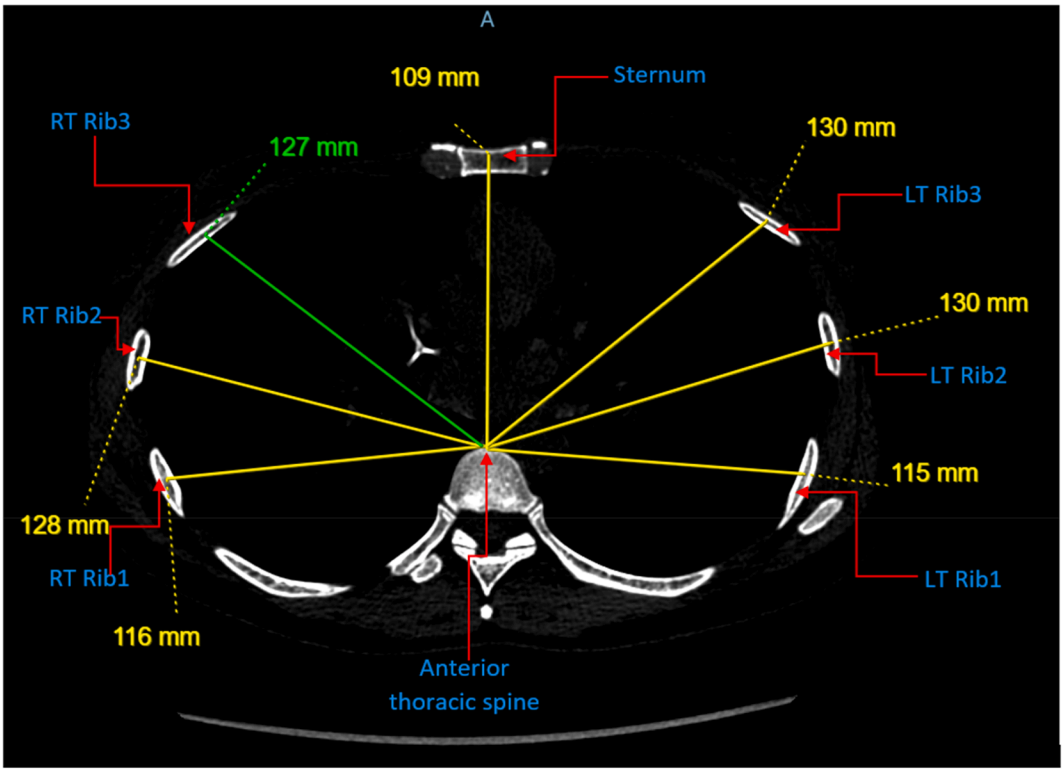

Figure 3. An axial computed tomography (CT) image showing the measurements of each rib landmark points in a healthy female. The measurements started from the anterior thoracic spine and ended at the centre or tip of each of the three rib landmark points on the left and right side of the sternum. The measurement of the sternum started from the anterior thoracic spine and ended at the centre or tip of the sternum. Abbreviation: RT, right; LT, left; mm, millimetre.

government organizations.[27–30] Formally, a BN model is a graphical representation, i.e., a directed acyclic graph (DAG), of a joint probability distribution of a set of random variables in which each variable is represented by a node and the dependency relationship is represented by a link/edge for two associated variables.[27,28] Bayesian Network was so named because it can be considered as a mechanism for automatically applying Bayes' theorem to complex problems. The Bayes Theorem (or Bayes Rule) is a mathematical statement which expresses the interrelationships between the conditional, marginal, and joint probability distributions of random variables as defined in the following formula[28]:

$$\Pr(B|A) = \frac{\Pr(A|B)\Pr(B)}{\Pr(A)} = \frac{\Pr\ (A,B)}{\Pr\ (A)},$$

where,

- A and B are two random variables/events;
- Pr(A) and Pr(B) are the marginal probability distributions of A and B, respectively;
- Pr(B|A) is the conditional probability distribution of B given A;
- Pr(A|B) is the conditional probability distribution of A given B; and
- Pr(A, B) is the joint probability distribution of A and B.

In a complex model that involves many variables, through the Bayes Theorem, a BN model quantifies the local dependency relationships between a variable (node) and its parent variables (nodes).[27,28] Then all local dependency relationships are integrated based on the probability chain rule so that the joint distribution of the global (i.e., overall) interrelationships among all variables can be determined/characterised.[27,28] Fig. 3 showed the pink-coloured nodes corresponding to the sectional layout of measurement scheme and Fig. 4 presented the derived BN model of female rib cage size and quantified categories of body habitus.

While the traditional regression analyses allow us to examine an outcome/dependent variable is associated with one or more predictor/independent variables under a conditional probability distribution framework, a BN model enables a researcher to investigate the associations between any subset of variables and the remaining variables in the model.[28,31] More specifically, a BN model enables inferential 'scenario analysis' by fixing the values of selected variables and predicting the values of the remaining variables. That is, any variable(s) (the basis for defining a scenario) can be selected to analyse the remaining variables in the model. Hence, the interactive BN model allows for various inferential analyses to be performed by assuming different scenarios in terms of the 'findings' of other variables. To answer the research questions of this study, scenario analyses were performed to investigate the patterns of the female rib cage size (RT Rib 1, RT Rib 2, RT Rib 3, Sternum, LT Rib 3, LT Rib 2, LT Rib 1). The analysis results have been numerically summarised in Table 1. Some examples pictures were provided in Appendix to show the details of how the numeric values presented in Table 1 could be extracted from the BN scenario analysis. Descriptive statistics were also required to summarise other numerical characteristics of the data set, including age category.[32] Majority of the chest images reflect White Caucasian (74.9 %) and Black or African American (19.3 %) females aged 40–89 years (Fig. 4). Female rib cages were categorised into three types with quantified percentages; lean (20.5 %); norm (55.6 %) and curvaceous (23.9 %) (Fig. 4). The classification into three body types was derived from a Multiple

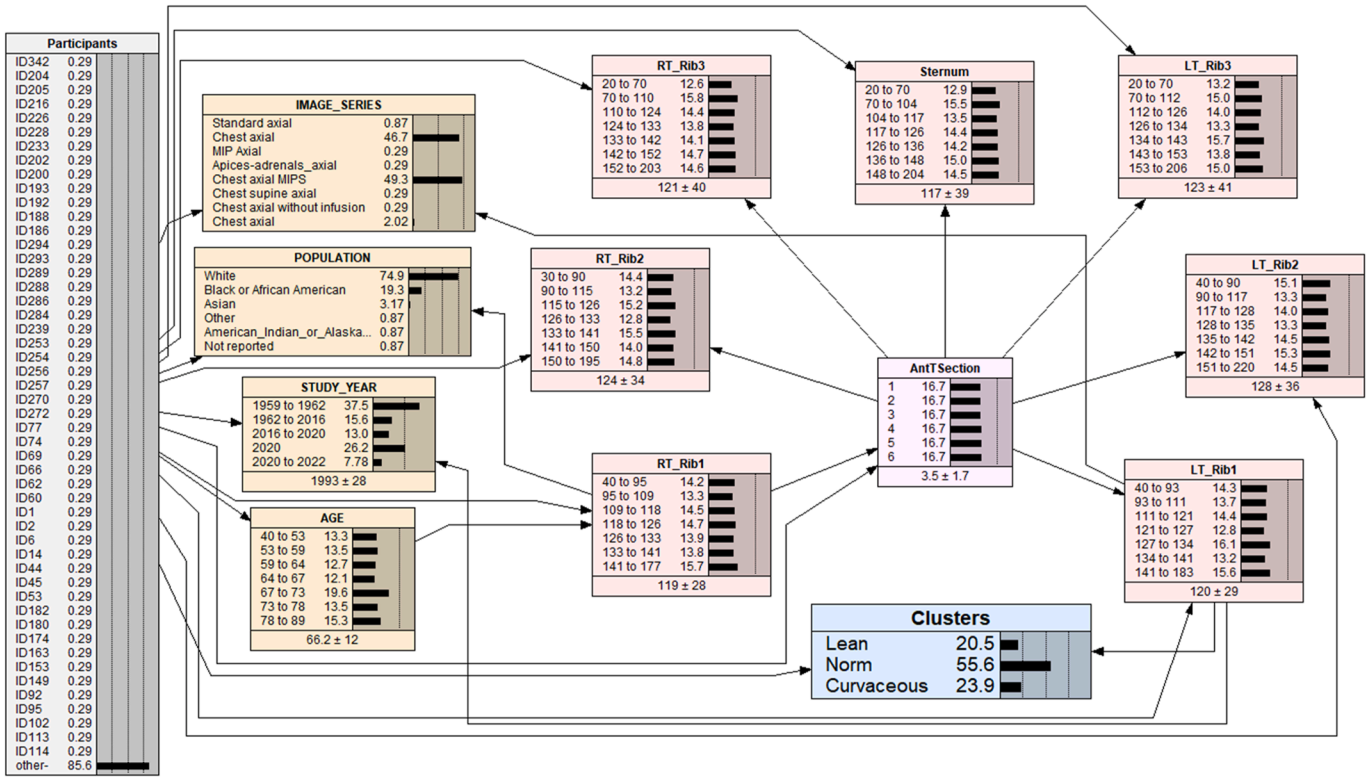

Figure 4. A Bayesian Network (BN) model of female rib cage size and quantified categories of body habitus. Each variable in a BN model is represented by a node. The link between two nodes represents the dependency relationship between two variables. The middle column of each node is a percentage totalling 100 %, representing the analysis outcomes of each level within a node. The last column is a graphical representation of the percentage values for each level, which are shown as distribution bars. The vertical dotted lines are markers, which are equally spaced to aid in visualising the comparative heights of the distribution bars. Abbreviation: RT, right; LT, left; AntTSection, Anterior thoracic section.

Correspondence Analysis (MCA) performed in R,[33] and the resulting classifications were used as one of the variables in the development of the BN model. The classification criterion in MCA is based on minimizing within-cluster inertia and maximizing between-cluster inertia.[34]

Discussion

Based on the 347 images that were retrieved in this study, the development of the BN model has followed the sampling-subject-oriented approach with the image's ID as the target variable for the specification of the model structure[30] and the most widely used and scholarly accepted commercial BN software package Netica was employed to build the BN model.[35] As argued in Xie et al.,[30] the BN model derived from the sampling-subject-oriented approach best represents the information contained in the image data in the sense that the model's in-sample prediction results have a minimal error rate assessed by Netica's 'Test With Cases' function.[35] Fig. 4 presented the derived BN model of female rib cage size and quantified categories of body habitus. As shown in Fig. 4, the BN model included 14 nodes/variables, and the pink-coloured nodes corresponded to the sectional layout of measurement scheme shown in Fig. 3. The information of the 347 female thorax images was compactly summarised in the eight pink-coloured nodes in Fig. 4. It showed that seven numeric measures (length and curvature) of the thorax using CT chest images (RT Rib 1, RT Rib 2, RT Rib 3, Sternum, LT Rib 3, LT Rib 2, LT Rib 1) were taken at each one of the six levels of the anterior thoracic spine sections. The measurement values of each of the seven variables had been divided into seven roughly evenly distributed intervals and the mean and standard deviation values were shown in the bottom part of each node. The splitting of each numeric variable into seven groups was done to determine the length and curvature of the thorax. The classification into three body types was derived from a Multiple Correspondence Analysis (MCA) performed in R[34] and the resulting classifications were used as one of the variables in the development of the BN model. The classification criterion in MCA is based on minimising within-cluster inertia and maximising between-cluster inertia.[34]

The Bayesian network (BN) model in this study can be used as a decision-making tool to facilitate the screening and diagnostic settings to implement in BS facilities. For example, given a set of new measurement values (RT Rib 1, RT Rib 2, RT Rib 3, Sternum, LT Rib 3, LT Rib 2, LT Rib 1), the BN model can return the best estimated categorisation result (Lean, Norm, or Curvaceous) for the image case in concern. In the present study, female body habitus (thoracic sizes) were quantified into three categories (Fig. 4): Lean (20.5 %); Norm (55.6 %) and Curvaceous (23.9 %). The categories for normal female body habitus (55.6 %) are almost similar to 50 % of the total human body habitus reflecting the sthenic (average/normal) body habitus.[14] This finding is novel since it demonstrates that more than half of the normal female body habitus falls under the same category as the normal human body habitus in a larger population. The categories for lean female body habitus (20.5 %) and curvaceous or wider female body habitus (23.9 %) greatly differs from the total human body habitus category (asthenic [lean] = 10 % vs hypersthenic [wider] = 5 %), respectively as defined by radiography text.[12,14] The difference in these findings could partly be influenced by gender differences (male vs female), age differences, total population and the approach used in quantifying the thoracic sizes.[18,19,36,37] Despite these differences, results of the present study facilitated a good understanding of the range of female body habitus (thoracic size) to improve mammography positioning practice and maximise image quality. Establishing a

Table 1
The Bayesian Network (BN) model estimated mean values and the corresponding 80 % prediction interval ranges for the healthy female rib cage size.

	AntTSection	RT_Rib1	RT_Rib2	RT_Rib3	Sternum	LT_Rib3	LT_Rib2	LT_Rib1
Lean (mean)	1	74.6	64.2	51.3	49.5	49.5	68.3	72.0
Lean (80 % interval)	1	(46.9, 103.1)	(36.7, 89.9)	(25.8, 81.6)	(25.5, 69.9)	(25.5, 69.9)	45.5, 89.2)	(46.3, 99.4)
Norm (mean)	1	76	65.9	54.8	53.7	53.6	69	72.8
Norm (80 % interval)	1	(47.3, 103.4)	(37.0, 97.1)	(26.4, 91.6)	(26.3, 87.6)	(26.1, 89.5)	(45.6, 91.0)	(46.4, 101.0)
Curvaceous (mean)	1	79.4	76.7	70	72	70.5	78.2	80.3
Curvaceous (80 % interval)	1	(48.0, 108.8)	(39.8, 109.1)	(30.9, 103.4)	(32.6, 101.5)	(30.9, 105.0)	(47.5, 109.7)	(48.5, 107.6)
Lean (mean)	2	102	103	93.7	91.4	92.2	103	102
Lean (80 % interval)	2	(72.6, 120.3)	(77.4, 123.2)	(70.9, 120.7)	64.4, 119.1)	(64.4, 122.7)	(75.5, 126.9)	(66.9, 123.3)
Norm (mean)	2	107	113	104	103	105	112	109
Norm (80 % interval)	2	(96.2, 121.3)	(94.9, 128.2)	(77.6, 125.0)	(77.2, 123.9)	(77.5, 127.1)	(94.1, 127.5)	(95.6, 121.9)
Curvaceous (mean)	2	113	124	129	126	129	126	115
Curvaceous (80 % interval)	2	(97.6, 130.1)	(104.8, 138.4)	(110.2, 143.8)	(105.8, 145.1)	(112.8, 147.8)	(107.2, 140.9)	(98.7, 130.0)
Lean (mean)	3	113	118	117	113	120	120	116
Lean (80 % interval)	3	(98.0, 126.0)	(98.5, 134.0)	(84.6, 140.1)	(82.4, 134.6)	(89.5, 139.9)	(96.2, 139.9)	(97.6, 131.3)
Norm (mean)	3	119.6	130	134	131	137	134	124
Norm (80 % interval)	3	(109.0, 131.2)	(117.2, 141.8)	(118.1, 148.9)	(112.0, 146.8)	(122.4, 150.7)	(121.0, 145.7)	(112.2, 135.4)
Curvaceous (mean)	3	129	150	163	159	166	154	132
Curvaceous (80 % interval)	3	(112.9, 140.9)	(134.4, 179.4)	(141.2, 194.2)	(131.9, 194.3)	(140.6, 197.4)	(133.8, 196.1)	(113.5, 161.2)
Lean (mean)	4	119	123	123	113	123	125	121
Lean (80 % interval)	4	(104.5, 133.9)	(115.0, 136.3)	(110.9, 140.1)	(86.0, 127.8)	(112.5, 138.9)	(108.3, 139.4)	(111.4, 132.9)
Norm (mean)	4	131	140	143	134	143	145	134
Norm (80 % interval)	4	(118.6, 140.8)	(128.0, 149.1)	(126.4, 160.2)	(114.3, 147.6)	(128.2, 152.8)	(130.7, 156.6)	(121.2, 150.6)
Curvaceous (mean)	4	143	165	171	165	173	171	143
Curvaceous (80 % interval)	4	(121.8, 168.9)	(142.7, 188.9)	(145.0, 196.7)	(136.2, 196.3)	(146.9, 199.5)	(142.1, 209.4)	(119.6, 173.6)
Lean (mean)	5	123	124	116	107	117	125	125
Lean (80 % interval)	5	(109.1, 135.3)	(103.9, 137.6)	(85.3, 134.6)	(78.7, 127.5)	(86.0, 134.0)	(103.7, 141.0)	(111.6, 136.1)
Norm (mean)	5	142	148	143	136	144	148	140
Norm (80 % interval)	5	(123.6, 167.7)	(133.3, 177.3)	(126.3, 156.1)	(117.8, 157.0)	(127.9, 165.1)	(130.6, 183.0)	(124.5, 167.1)
Curvaceous (mean)	5	150	166	172	170	175	178	153
Curvaceous (80 % interval)	5	(133.9, 171.7)	(142.1, 189.3)	(147.3, 197.0)	(141.2, 197.3)	(150.6, 200.0)	(146.4, 211.6)	(130.3, 177.2)
Lean (mean)	6	124	117	106	100	110	121	123
Lean (80 % interval)	6	(109.1, 138.1)	(94.1, 136.5)	(75.5, 129.7)	(72.2, 125.3)	(76.9, 135.6)	(96.9, 139.6)	(103.0, 137.9)
Norm (mean)	6	141	143	135	129	138	147	142
Norm (80 % interval)	6	(123.3, 167.2)	(126.2, 172.7)	(114.7, 150.6)	(108.1, 146.8)	(117.9, 152.3)	(127.6, 184.0)	(125.0, 170.3)
Curvaceous (mean)	6	150	160	161	156	162	172	154
Curvaceous (80 % interval)	6	(130.6, 171.6)	(133.9, 188.2)	(128.1, 194.5)	(127.8, 193.7)	(131.3, 196.6)	(138.8, 210.1)	(130.8, 177.4)
Lean (mean)	**Average**	109	108	101	95.7	102	110	110
Lean (80 % interval)	**Average**	(71.3, 131.5)	(61.6, 133.5)	(48.8, 133.4)	(46.3, 125.4)	(47.0, 133.8)	(66.0, 136.8)	(68.2, 132.4)
Norm (mean)	**Average**	120	123	119	115	120	126	120
Norm (80 % interval)	**Average**	(80.1, 151.6)	(71.4, 149.4)	(58.3, 149.7)	(57.4, 145.5)	(56.6, 150.8)	(72.7, 150.1)	(77.2, 148.3)
Curvaceous (mean)	**Average**	127	140	144	141	146	147	130
Curvaceous (80 % interval)	**Average**	(84.9, 165.5)	(88.6, 184.1)	(79.1, 192.4)	(81.2, 191.7)	(79.7, 195.0)	(85.3, 203.2)	90.8, 171.0)

Abbreviation: RT, right; LT, left; AntTSection, Anterior thoracic section. Note: Light gold colour represents the average female thorax size at each one of the six levels of the anterior thoracic spine sections revealing slight variations in rib cage dimensions.

range of female thoracic sizes supports understanding of best practice positioning of females that do not fit the 'norm' in terms of body habitus.

The Bayesian network (BN) model in the present study estimated mean values and the corresponding 80 % prediction interval ranges for the healthy female rib cage size (Table 1, Fig. 3). The average female thorax size at each one of the six levels of the anterior thoracic spine sections revealed slight variations in rib cage dimensions (Table 1): RT Rib1 = 120 mm; RT Rib2 = 123 mm; RT Rib3 = 119 mm; Sternum = 115 mm; LT Rib3 = 120 mm; LT Rib2 = 126 mm; and LT Rib1 = 120 mm. These slight variations in female rib cage dimensions could reflect the slow changes in the growth of each rib overtime but do not reflect the true thoracic sizes of male, children or adult individuals with chest wall deformities.[38] These findings differ from previous studies[36,37] investigating the impact of human characteristics on rib cage geometry. Kent et al.[37] revealed a significant relationship between rib angle, age and body mass index (BMI) from CT scans of 161 patients. Another study by Gayzik et al.[36] developed a statistical model for quantifying the age-related rib cage shape change using landmark data from 63 male subjects. Their study found that older males generally had flatter rib angles and greater kyphosis on the thoracic spine. Furthermore, Shi et al.[19] identified 464 landmarks on each of their 89 subjects and revealed significant effects on rib cross-sectional area using a linear mixed model except for BMI. The difference of results in these studies[19,36,37] compared to the present study relates to the total population studied and the approach used in measuring the rib cage dimensions. The present study used BN model to quantify rib cage dimensions of a larger female population ($n = 347$) aged 40–89 years reflective of a mammography screening population[20,21] whilst these same studies[19,36,37] used 2D and 3D geometry calculations of both adult male and female rib cage of a smaller population. Whilst these differences are crucial for these previous studies[19,36,37] in addressing their study aim, the results in the present study are also significant in that it evidences for the first time the true range of thoracic profiles of a larger female population. This novel finding supports understanding of best mammography positioning practices to minimise the impact of missing breast tissue and enhances breast cancer detection.

This is the first study establishing the true range of female thoracic sizes and quantified female body habitus in a larger population and adds to the limited body of knowledge in radiography. The use of a BN approach is superior in predicting the quantified female thoracic profile to compare with the established range of the total human body habitus categories defined by radiography educational text.[12,14] However, this is a typical

observational study based on a convenience sample of 347 CT images. Hence, the limitation in the study acknowledges that the majority of the female population reflect White Caucasian and Black or African American females aged 40–89 years and results may not represent a true wider global female population. Finally, demographics are not the focus of this study but may be noted as a confounding factor impacting the interpretation of the analysis results of this study.

Conclusion

The significance of this study is that it categorised 55.6 % of female thoracic sizes as being normal on a larger group of female population. A BN model was used to quantify thoracic sizes of a larger female population aged 40–89 years reflective of a mammography screening population. A better understanding of the impact of the thorax on image quality will support improved positioning practice and improved accuracy for breast cancer diagnosis. A lack of body habitus criteria in image evaluation system (IES) highlights an urgent need for screening and diagnostic settings to implement in BS facilities. This range of thorax sizes should be integrated as a body habitus criterion in the current IES to maximise image quality and enhance subsequent breast cancer diagnosis.

The current analysis results are based on one set of sample data. Hence, the same study should be repeated in different areas by different research team by following the same protocol of the study design and modelling approach. By collecting multiple set of sample data for the quantification and classification of female's body habitus, the current modelling results can be updated accordingly and the validity of the generalisation of the analysis results will be better established/further consolidated. Whilst demographic limitations are acknowledged, the lack of ethnic diversity and the exclusion of certain chest conditions limit broader applicability. These issues could be further explored in future research. The BN model in this study can be used as a decision-making tool to facilitate the screening and diagnostic settings to implement in BS facilities. Further study on how thoracic size directly correlates with image quality in CC and MLO view using practical mammography datasets is highly recommended. While this study quantified a range of female body habitus categories, further research is needed to determine the impact of the thorax size and how this impacts breast tissue inclusion during CC and MLO positioning.

Informed consent

The CT chest images used in this work are in public domain, and access to these databases was approved by the database owners. As such, informed consent was obtained before data collection by the respective database owners.

Author contributions

RP: Conceptualisation, Methodology, Visualisation, Formal analysis, Investigation, Writing - original draft, Writing - review & editing.

GX: Methodology, Software, Validation, Formal analysis, Writing – review & editing.

XZ: Supervision, Formal analysis, Writing – review & editing.

AC: Supervision, Writing - review & editing.

CW: Supervision, Writing - review & editing.

CC: Supervision, Writing - review & editing.

All authors have read and agreed to the published version of the manuscript.

Ethics approval and consent to participate

The CT chest images used in this work are in public domain, and access to these databases was approved by the database owners. As such: (1) the institutional ethics approval was exempted by Charles Sturt University's Human Research Ethics Committee; (2) the methods used in this study are in accordance with the guidelines of Charles Sturt University's Human Research Ethics Committee.

Availability of data

The original CT chest image data were downloaded from the Medical Imaging and Data Resource Center (MIDRC) database (https://www.midrc.org) (accessed on 16 January 2024). The processed data and the BN model dataset required for this study may be made available by the author(s) upon reasonable request.

Generative AI use

Not applicable.

Funding

This research was funded through the Australian Awards Scholarship as part of the first author's (RP) PhD Program at Charles Sturt University. The author very much appreciates and acknowledges the Australian Award Scholarship for funding this doctoral research study.

Conflict of interest statement

None.

Acknowledgements

CT chest data used in preparation of this article were obtained from the Medical Imaging and Data Resource Center (MIDRC) database (https://www.midrc.org). As such, the investigators within the MIDRC contributed to the design and implementation of MIDRC and/or provided data but did not participate in analysis or writing of this report. A complete listing of MIDRC investigators can be found at: https://www.midrc.org/midrc-team.

Appendix A. Supplementary data

Supplementary data to this article can be found online at https://doi.org/10.1016/j.radi.2025.103020.

References

1. World Health Organisation. *Globocan 2020: new global cancer data*. 2020. Available at: https://www.uicc.org/news/globocan-2020-new-global-cancer-data.
2. World Health Organisation. *WHO position paper on mammography screening*. WHO Press; 2014. Available at: https://www.who.int/publications/i/item/who-position-paper-on-mammography-screening.
3. Tabár L, Tot T, Dean PB. A new era in the diagnosis and treatment of breast cancer. In: Tabár L, Tot T, Dean PB, editors. *Breast cancer: the art and science of early detection with mammography. Perception, interpretation, histopathologic correlation*, vol. 1. Stuttgart: Georg Thieme Verlag; 2005. p. 166–235.
4. Garnett SE. Male mammography. In: Hogg P, Kelly J, Mercer C, editors. *Digital mammography: a holistic approach*. Springer International Publishing; 2015. p. 239–40. https://doi.org/10.1007/978-3-319-04831-4_1.
5. National Health Service Breast Cancer Screening Program. *National quality assurance coordinating group for radiography: quality assurance guidelines for mammography including radiographic quality control*. NHS Cancer Screening Programmes; 2006 (Publication No. 63).

6. Long SM, Miller LC, Botsco MA, Martin LL. *The handbook of mammography*. 5th ed. Mammography Consulting Services Ltd; 2010.
7. Brown M, Eccles C, Wallis M. Geographical distribution of breast cancers on the mammogram: an interval cancer database. *Br J Radiol* 2001;**74**(880): 317–22. https://doi.org/10.1259/bjr.74.880.740317.
8. Handley R. Carcinoma of the breast. *Ann R Coll Surg Engl* 1975;**57**(2):59. https://pmc.ncbi.nlm.nih.gov/articles/PMC2388579/.
9. Tabar L. *Teaching course in diagnostic breast imaging: finding breast cancer in early stages - detection, diagnosis and implication for management*. Mammography Education, Inc; 2004.
10. Cardenosa G. In: McAllister L, Barrett K, editors. *Breast imaging companion*. 3rd ed. Lippincott Williams & Wilkins; 2008.
11. MIDRC. *Medical imaging and data resource center*. 2025. https://www.midrc.org. [Accessed 13 January 2025].
12. Hardy M, Scotland B, Herron L. Assessing sagittal rotation on posteroanterior chest radiographs: the effect of body morphology on radiographic appearances. *J Med Imag Radiat Sci* 2015;**46**(4):365–71. https://doi.org/10.1016/j.jmir.2015.07.004.
13. Bentley K, Poulos A, Rickard M. Mammography image quality: analysis of evaluation criteria using pectoral muscle presentation. *Radiography* 2008;**14** (3):189–94. https://doi.org/10.1016/j.radi.2007.02.002.
14. Bontrager KL, Lampignano JP. *Textbook of radiographic positioning and related anatomy*. Mosby Inc, Elsevier Inc; 2014.
15. Harati K, Kolbenschlag J, Behr B, Goertz O, Hirsch T, Kapalschinski N, et al. Thoracic wall reconstruction after tumor resection. *Front Oncol* 2015;**5**:247. https://doi.org/10.3389/fonc.2015.00247.
16. Uemura S, Yoshida A, Kuyama H. Analysis of chest wall elevation after the Nuss procedure using 3D body scanning technique in patients with pectus excavatum. *Pediatr Surg Int* 2021;**37**(6):777–82. https://doi.org/10.1007/s00383-021-04885-3.
17. Akil A, Ziegeler S, Reichelt J, Semik M, Müller MC, Fischer S. Rib osteosynthesis is a safe and effective treatment and leads to a significant reduction of trauma associated pain. *Eur J Trauma Emerg Surg* 2019;**45**(4):623–30. https://doi.org/10.1007/s00068-018-01062-5.
18. Pickard A, Darby M, Soar J. Radiological assessment of the adult chest: implications for chest compressions. *Resuscitation* 2006;**71**:387–90. https://doi.org/10.1016/j.resuscitation.2006.04.012.
19. Shi X, Cao L, Reed MP, Rupp JD, Hoff CN, Hu J. A statistical human rib cage geometry model accounting for variations by age, sex, stature and body mass index. *J Biomech* 2014;**47**(10):2277–85. https://doi.org/10.1016/j.jbiomech.2014.04.045.
20. Australian Institute of Health and Welfare. *BreastScreen Australia monitoring report 2014-2015. (Cancer Series no. 106)*. Australian Institute of Health and Welfare; 2017. Available at: https://www.aihw.gov.au/getmedia/04ac86ad-666f-4004-ad33-7c5c3c3f9260/20460.pdf.aspx?inline=true.
21. Cancer Institute NSW. *BreastScreen NSW*. 2023. Available at: https://www.cancer.nsw.gov.au/research-and-data/cancer-data-and-statistics/data-available-now/cancer-statistics-nsw/breastscreen-nsw.
22. Calculator.net. *Sample size calculator*. 2023. Available at: https://www.abs.gov.au/websitedbs/d3310114.nsf/home/sample+size+calculator.
23. Haje SA, Haje DP. Overcorrection during treatment of pectus deformities with DCC orthoses: experience in 17 cases. *Int Orthop* 2006;**30**(4):262–76. https://doi.org/10.1007/s00264-005-0060-0.
24. Schwabegger AH, Del Frari B. Surgery of other congenital anomalies of the anterior thoracic wall. *Cong Thorac Wall Deform: Diagn Ther Curr Develop* 2011: 267–76. https://doi.org/10.1007/978-3-211-99138-1_11.
25. Wachter T, Del Frari B, Edlinger M, Morandi EM, Mayerl C, Verstappen R, et al. Aesthetic outcomes after surgical repair of pectus excavatum in females: differences between patients and professional evaluators. *Arch Plast Surg* 2020;**47**(2):126–34. https://doi.org/10.5999/aps.2019.00318.
26. R Core Team. *R: a language and environment for statistical computing*. Vienna, Austria: R foundation for statistical comupting; 2022., version 4.2.2.
27. Pearl J. *Probabilistic reasoning in intelligent systems*. San Mateo, CA: Morgan Kaufmann; 1988. https://doi.org/10.2307/2275238.
28. Kjærulff UB, Madsen AL. *Bayesian networks and influence diagrams: a guide to construction and analysis*. Cham: Springer; 2008. Available at: https://link.springer.com/book/10.1007/978-0-387-74101-7.
29. Pandey S, Johnson AC, Xie G, Gurr GM. Pesticide regime can negate the positive influence of native vegetation donor habitat on natural enemy abundance in adjacent crop fields. *Front Ecol Evol* 2022;**10**:815162. https://doi.org/10.3389/fevo.2022.815162.
30. Xie G, Wang B, Manyweathers J. A novel Bayesian Network modelling approach that can ideally represent the information contained in a set of sample data. *SocArXiv* 2023. https://doi.org/10.31235/osf.io/gqud3. Preprint published in.
31. Kruschke JK. Bayesian analysis reporting guidelines. *Nat Hum Behav* 2021;**5** (10):1282–91. https://doi.org/10.1038/s41562-021-01177-7.
32. Riffenburgh RH. *Statistics in medicine. 3rd ed. Clinical investigation department. Naval medical centre*. San Diego, California, United States of America: Elservier Inc; 2012. https://doi.org/10.1016/B978-0-12-384864-2.00005-6.
33. Lê S, Josse J, Husson F. FactoMineR: an R package for multivariate analysis. *J Stat Software* 2008;**25**(1):1–18. https://doi.org/10.18637/jss.v025.i01.
34. Husson F, Le S, Pages J. *Exploratory multivariate analysis by example using R*. 2nd ed. New York, United States of America: CRC Press; 2017. https://doi.org/10.1201/b21874.
35. *Netica 64 bit (for windows 7 to 10) [computer program]*. Vancouver, BC: Norsys Software Corp; 2021., Version 6.09.
36. Gayzik FS, Yu MM, Danelson KA, Slice DE, Stitzel JD. Quantification of age-related shape change of the human rib cage through geometric morphometrics. *J Biomech* 2008;**41**(7):1545–54. https://doi.org/10.1016/j.jbiomech.2008.02.006.
37. Kent R, Lee SH, Darvish K, Wang S, Poster CS, Lange AW, et al. Structural and material changes in the aging thorax and their role in crash protection for older occupants. *Stapp Car Crash J* 2005;**49**:231–49. https://doi.org/10.4271/2005-22-0011.
38. Blanco FC, Elliott ST, Sandler AD. Management of congenital chest wall deformities. *Semin Plast Surg* 2011;**25**(1):107–16. https://doi.org/10.1055/s-0031-1275177. Thieme Medical Publishers.